ACTIVE 2006
18-20 SEPTEMBER 2006
ADELAIDE AUSTRALIA

Zero-stiffness magnetic springs for active vibration isolation

Will Robertson[a], Rohin Wood, Ben Cazzolato, Anthony Zander
School of Mechanical Engineering
University of Adelaide, SA
Australia 5005

ABSTRACT

Active vibration isolation of large load structures typically requires significant actuator energy. With a zero stiffness support, which can be realised with a permanent magnet system, reactive forces may be applied to the structure with comparatively little effort. This paper presents simulation results for such a magnetic spring arrangement which is stabilised by a non-linear controller. Transmissibility less than unity is demonstrated over the entire frequency spectrum.

1 INTRODUCTION

In a large load vibration isolation system, significant static forces are required to counter the effects of gravity. For a conventional linear isolator, this compensating force is $F = -kx_0$, for stiffness k and static deflection x_0. Accordingly, for large forces the stiffness and/or the static deflection must also be large.

While low stiffness is advantageous for vibration isolation, there is a practical lower limit on obtaining a stiffness to support a large load. The disadvantage of increasing the stiffness of the system is due to the corresponding increase in the resonant frequency $\omega_n = \sqrt{k/m}$, for mass m. This results in poor passive vibration isolation for frequencies below $\sqrt{2}\cdot\omega_n$. Accordingly, a method of supporting large loads while keeping the stiffness low is desirable. For an active system, it will be shown that, in this case, the further advantage is gained of reduced control effort in actuating the device.

In this paper, a permanent magnetic configuration is demonstrated that can reduce the passive stiffness to zero at unstable equilibrium while still providing a supporting force. The magnetic design is scalable, which provides for the capability of large load bearing. Non-linear control laws are proposed to stabilise the system and are demonstrated via simulation. Finally, implementation issues are discussed for a practical system.

2 PERMANENT MAGNET SPRINGS

The simplest form of magnetic suspension is the vertically attractive pair in Figure 1a, in which a fixed upper magnet supports the lower in an unstable manner. Due to the inherent instability resulting from negative stiffness and the non-linear forces involved, this system is often used for demonstrations of the efficacy of active control techniques.

While all permanent magnet levitations are unstable by nature [1, 2], in a completely passive magnetic spring instability in directions other than the supporting direction can be controlled with rigid guides (for example, see the isolator of Puppin and Fratello [3]). Such a configuration, shown in Figure 1b, consists of a vertical pair of magnets in repulsion, with the lower magnet providing the supporting forces.

Zero stiffness structures for vibration isolation from the ground have been examined by Nijsse [4], who introduced the magnet arrangement shown in Figure 1c, a combination

[a]Email address: will@mecheng.adelaide.edu.au

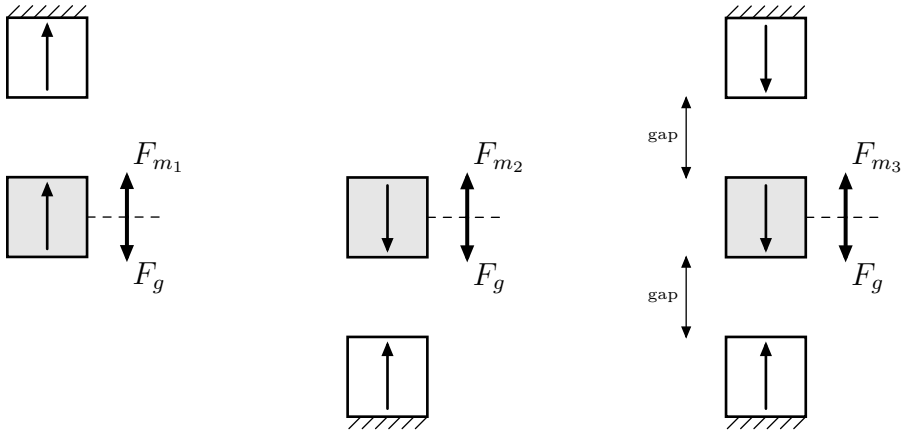

(a) Vertically attracting spring (b) Vertically repelling spring (c) Combination spring

Figure 1: Magnetic springs for bearing vertical loads. The shaded magnet in each is supported against gravity (F_g) by the respective magnetic forces (F_{m_i}). Arrows within the magnets indicate their directions of magnetisation.

of the two aforementioned magnetic springs. Xing et al. [5] have examined the general solution for feedback control systems achieving zero and infinite stiffness.

This paper further develops the concept of zero stiffness through the parallel combination of two magnetic springs, $k = k_1 + k_2 = 0$, via theoretical modelling and simulated non-linear control.

3 ZERO STIFFNESS

The term 'zero stiffness' strictly denotes a decoupling between displacement and force for two disparate objects in space;

$$F(x) = \lim_{k \to 0} -kx = 0. \tag{1}$$

However, for any practical quasi-zero stiffness system (also see the mechanically zero stiffness spring of Carrella et. al [6]) the stiffness varies by position, so perturbations from the equilibrium point eliminate the zero stiffness property. On the other hand, small perturbations lead only to small changes in the stiffness, which will therefore remain close to zero.

Taking the inverse of Eq. (1) naïvely implies that for a totally zero stiffness system, applied force will effect a displacement without bound: $x(F) = \lim_{k \to 0} -F/k = \infty$. In a more realistic case, the lower the stiffness the more easily the system can be actuated.

4 PERMANENT MAGNET DESIGN

In this section, the stabilities through displacement in the load bearing direction for the three springs shown in Figure 1 are analysed in order to show the desirable properties of the zero stiffness magnetic spring.

4.1 Mathematical models

Expressions for the forces between magnets follow directly from Maxwell's equations, and may be derived in a number of ways. For cuboid-shaped magnets with magnetisations in the z-direction that experience translation in three degrees of freedom but no rotation, a relatively concise analytical solution for the forces in each direction, $\boldsymbol{F} = [F_x, F_y, F_z]$, has been known for over twenty years [7]:

$$\boldsymbol{F} = \frac{JJ'}{4\pi\mu_0} \sum_{(i,j,k,l,p,q)\in\{0,1\}^6} \boldsymbol{f}(u_{ij}, v_{kl}, w_{pq}) \cdot [-1]^{i+j+k+l+p+q}\,, \tag{2}$$

where $\boldsymbol{f}(u, v, w) = [f_x, f_y, f_z]$ is defined by

$$\begin{aligned}
f_x &= \tfrac{1}{2}[v^2 - w^2]\ln(r-u) + uv\ln(r-v) + vw\arctan\!\left(\tfrac{uv}{rw}\right) + \tfrac{1}{2}ru,\\
f_y &= \tfrac{1}{2}[u^2 - w^2]\ln(r-v) + uv\ln(r-u) + uw\arctan\!\left(\tfrac{uv}{rw}\right) + \tfrac{1}{2}rv,\\
f_z &= -uw\ln(r-u) - vw\ln(r-v) + uv\arctan\!\left(\tfrac{uv}{rw}\right) - rw,
\end{aligned}$$

and

$$\begin{aligned}
u_{ij} &= \alpha - a[-1]^i + A[-1]^j\,,\\
v_{kl} &= \beta - b[-1]^k + B[-1]^l\,, \qquad r = \sqrt{u_{ij}^2 + v_{kl}^2 + w_{pq}^2},\\
w_{pq} &= \alpha - c[-1]^p + C[-1]^q\,,
\end{aligned}$$

where $[a, b, c]$ and $[A, B, C]$ are the half dimensions of the fixed and floating magnets, respectively, and $[\alpha, \beta, \gamma]$ is the distance between their centres; J and J' are the magnetisations, and μ_0 is the permeability of free space. Recently, equivalent methods have been demonstrated that provide more abstract methods for dealing with more complex geometries [8].

The solution shown in Eq. (2), and others like it, provide a convenient way to analyse the behaviour of any simple permanent magnet configuration. Since the coercivity of rare earth magnetic material is great enough to ensure that nearby magnets will not demagnetise each other, the forces follow the principle of superposition. That is, referring back to Figure 1, $F_{m_3} = F_{m_1} + F_{m_2}$.

Eq. (2) can be differentiated to obtain the stiffnesses, $\boldsymbol{K} = -\nabla_{xyz}\boldsymbol{F}$:

$$\boldsymbol{K} = \frac{JJ'}{4\pi\mu_0} \sum_{(i,j,k,l,p,q)\in\{0,1\}^6} \boldsymbol{k}(u_{ij}, v_{kl}, w_{pq}) \cdot [-1]^{i+j+k+l+p+q}\,, \tag{3}$$

where $\boldsymbol{k}(u, v, w) = [k_x, k_y, k_z]$ is defined by

$$\begin{aligned}
k_x = \kappa(u, v, w)\,, \quad k_y = \kappa(v, u, w)\,, \quad k_z = -k_x - k_y,\\
\kappa(u, v, w) = -\frac{vu^2}{u^2 + w^2} - r - v\log(r - v)\,,
\end{aligned}$$

and u, v, w, and r are as given in Eq. (2). Note that the result $k_x + k_y + k_z = 0$ follows from Earnshaw's theorem [1].

4.2 Stability analyses

The stability of a magnetic configuration may be investigated by examination of the stiffnesses in each direction, which may be calculated via application of Eq. (3). Stability exists for negative force gradients (positive stiffness), where the reaction forces act to oppose perturbatory displacements. In the following analyses, cube magnets of side length 20 mm are used with magnetisations of 1 T.

The stiffness in each translatory direction for the vertically attracting spring (Figure 1a) experiencing vertical deflection is shown in Figure 2. It can be seen that this spring is unstable (i.e., it has negative stiffness) in the vertical direction, but stable (positive stiffness) in both horizontal directions.

A similar analysis has been performed on the vertically repelling spring (Figure 1b), for which the results are displayed in Figure 3. These show opposite tendencies to the previous spring: both horizontal directions are unstable, but the vertical, load-bearing, direction is stable.

When these two springs are combined to create the spring shown in Figure 1c, the stiffnesses in each bearing direction have each a point of inflexion, as shown in Figure 4. This inflexion, equidistant between the two magnets, is the point of zero stiffness in both vertical and horizontal directions. The supporting force at this point is a function of the gap. This relationship is shown in Figure 5a, which plots vertical force vs. vertical displacement for a zero stiffness spring with varying gaps.

The curves shown in Figure 5b demonstrate the nominal load-bearing force of a zero stiffness spring with increasing cube magnet side-lengths. This figure indicates that a large design space is possible with appropriately chosen parameters.

5 CONTROL STRATEGIES

The basic zero stiffness configuration that is under examination is marginally stable at its operating point. The stable effects of the lower magnet and the unstable effects of the upper magnet combine to produce a unique force/displacement characteristic (zero slope) as seen in Figure 5a on the previous page.

To a good approximation, over the range of several millimetres this relationship may be modelled as quadratic: $F_m = Kx^2 + F_0$, for displacement x from the rest position at the point of zero stiffness, balanced midway between the two fixed magnets, with a supporting force F_0. When summed with the load due to gravity, this simplifies to $F = F_m - mg = Kx^2$.

For this stage of the analysis, the damping of the system is neglected, as its effect will be small. The approximate dynamic equation of motion of the zero stiffness spring is therefore (for mass m)

$$m\ddot{x} - Kx^2 = 0. \tag{4}$$

A controller for this unstable system may now be designed for the purposes of stable operation at the zero stiffness position. The design for a linear controller might proceed from here by (Jacobian) linearisation around the operating point; linear stiffness $k = \partial F/\partial x|_{x=0}$. This linearised system in state space form is

$$\begin{bmatrix} \ddot{x} \\ \dot{x} \end{bmatrix} = \begin{bmatrix} 0 & 0 \\ 1 & 0 \end{bmatrix} \begin{bmatrix} \dot{x} \\ x \end{bmatrix} + \begin{bmatrix} 1/m \\ 0 \end{bmatrix} u. \tag{5}$$

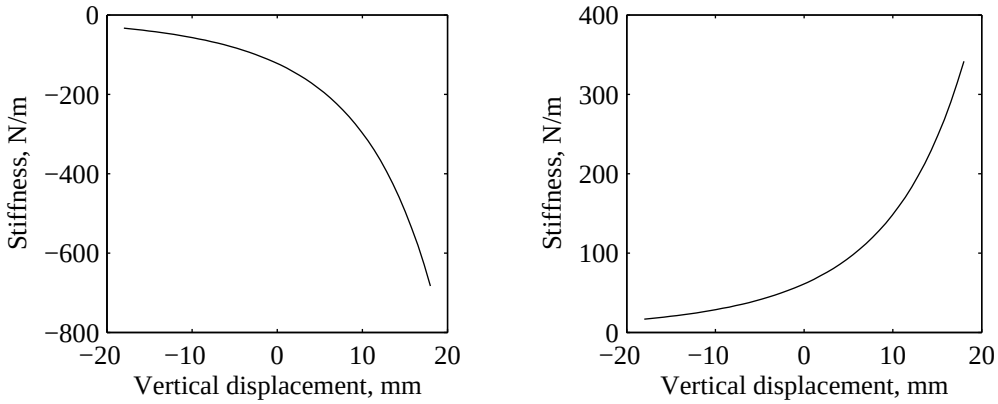

(a) Vertical stiffness (unstable) (b) Horizontal stiffnesses (stable)

Figure 2: Stiffnesses of the vertically attracting spring (Figure 1a).

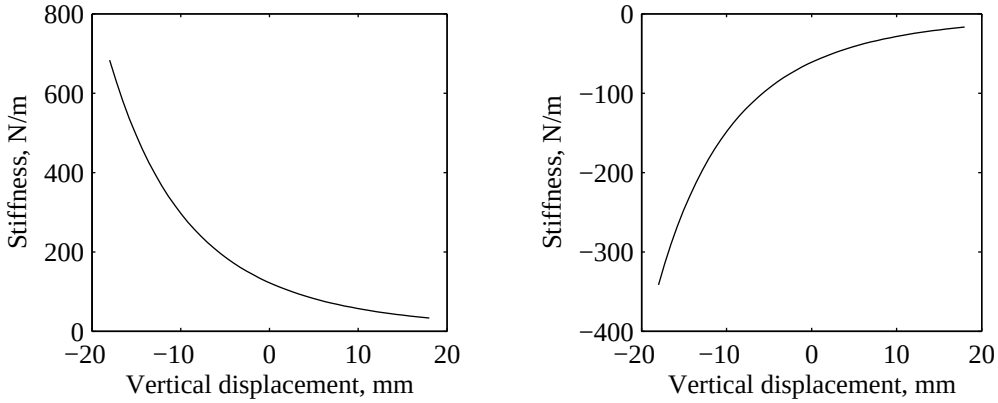

(a) Vertical stiffness (stable) (b) Horizontal stiffnesses (unstable)

Figure 3: Stiffnesses of the vertically repelling spring (Figure 1b).

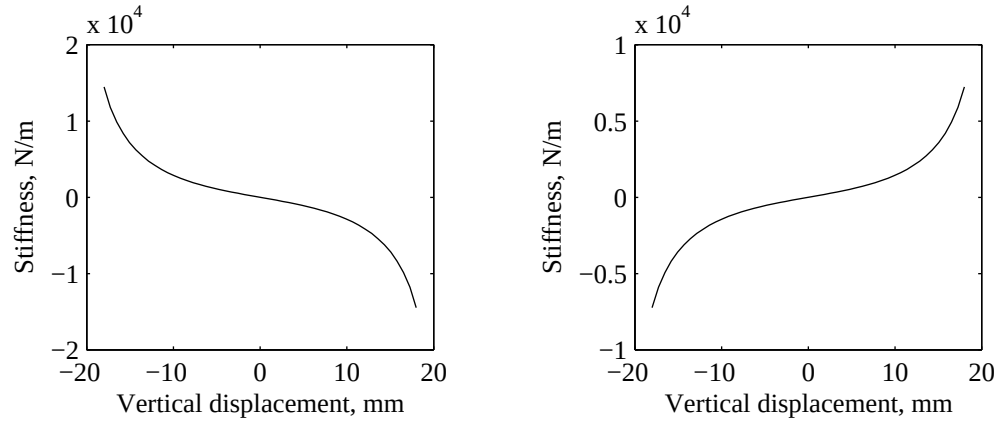

(a) Stiffness in the vertical direction (stable for negative displacements)

(b) Stiffnesses in the horizontal directions (stable for positive displacements)

Figure 4: Stiffnesses of the zero stiffness spring (Figure 1c).

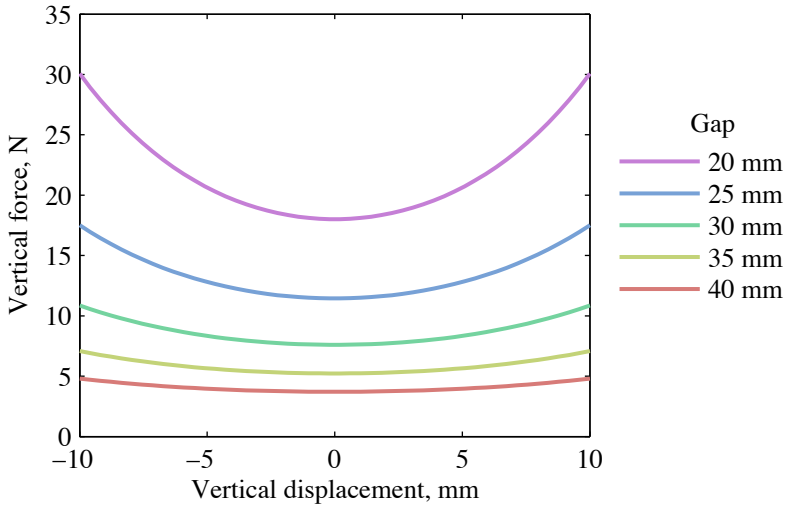

(a) Force/displacement curves for the magnetic arrangement shown in Figure 1c. 20 mm cube magnets are used with various gaps.

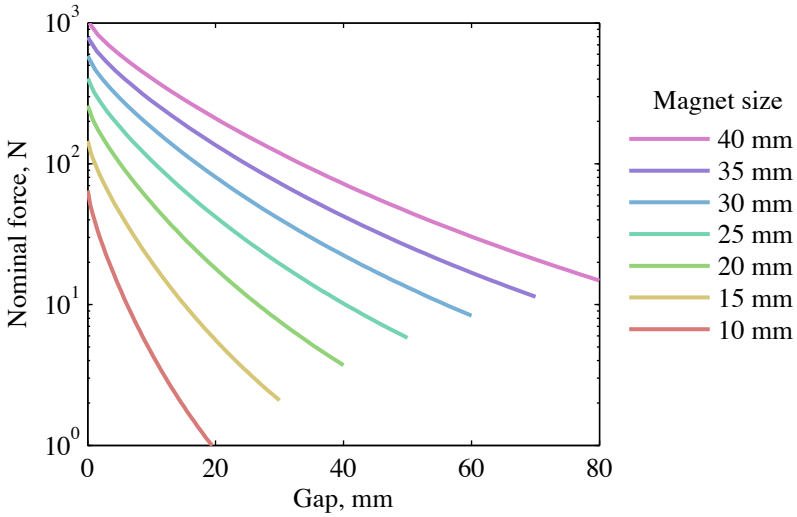

(b) Supporting force/gap curves for various magnet sizes at zero displacement. In each case, the gap range is 1–2 magnet dimensions. Increasing force results from increasing magnet size.

Figure 5: Dependence of the supporting force on geometry of the zero stiffness spring.

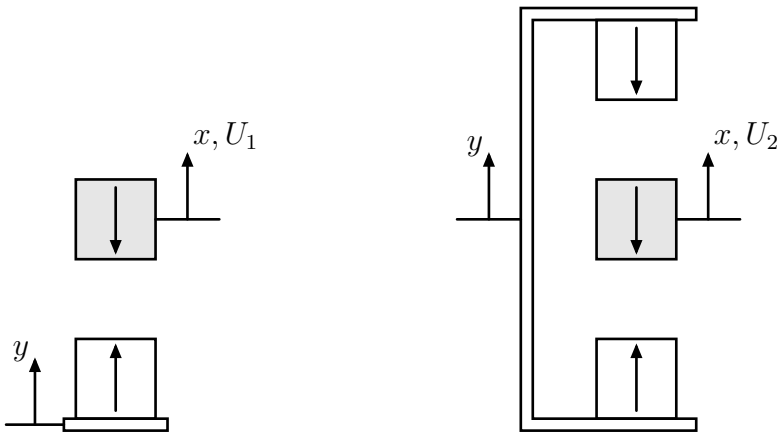

(a) Vertically repelling spring. (b) Zero stiffness spring.

Figure 6: Schematics of the simulated springs, for displacement x, disturbed by base excitation y, and controlled by input force U.

A standard linear controller designed around this model fails to stabilise the actual system robustly, due to the large gains that would be required to overcome the strong non-linear destabilising term. This can be shown using Lyapunov stability criterion [9]. Consequently, a simple backstepping controller [10] will be used that can accommodate such non-linear problems.

In order to compare the results from the controlled zero stiffness spring to a more conventional system, the same analysis will also be performed on the vertically repelling spring, which has behaviour similar to a standard linear spring. For the purposes of vibration isolation, it is desired to examine the vibration response due to indirect excitation through the (previously assumed fixed) base, representing undesirable ground vibration. Schematics for the two systems are shown in Figure 6, which defines U_1 and U_2 as inputs to the vertically repelling and zero stiffness springs, respectively.

The dynamic equation for these systems, assuming some linear viscous damping, d, and a non-linear stiffness force $F_k(\cdot)$, is

$$m\ddot{x} + d[\dot{x} - \dot{y}] - F_k(x - y) = U. \tag{6}$$

The actual forces $F_k(x - y)$ for each system may be calculated via application of Eq. (2). From such numerical results, approximations can be derived as follows for use in the control laws:

$$F_{k_1}(\bar{x}) \approx K_3\bar{x}^3 + K_2\bar{x}^2 + K_1\bar{x}, \qquad \text{(vertically repelling)} \tag{7}$$

$$F_{k_2}(\bar{x}) \approx K\bar{x}^2, \qquad \text{(zero stiffness)} \tag{8}$$

in which cancelation of the static force with the gravity load has been taken into account.

5.1 Controller derivation for the zero stiffness spring

The approximate non-linear system dynamics for the zero stiffness spring may be written in the following form:

$$\begin{aligned} \dot{x} &= v, \\ \dot{v} &= k[x-y]^2 + u, \end{aligned} \tag{9}$$

where x is the displacement state, v is the velocity state, $k = K/m$ from Eqs (4) and (8), and $u = U_2/m$ is the normalised input force.

An initial control Lyapunov function is chosen (typical for mechanical systems) around which to design a stability controller for the system:

$$V_1 \stackrel{\text{def}}{=} \tfrac{1}{2}x^2, \qquad\qquad \dot{V}_1 = x\dot{x} = xv.$$

The velocity term can now be considered (mathematically) as a virtual input for this system, $v = \xi + z$, where ξ is the desired value of v and z is the associated error:

$$\dot{V}_1 = x\xi + xz. \tag{10}$$

The term ξ is chosen such that the first term in Eq. (10) is negative definite:

$$\begin{aligned} \xi \stackrel{\text{def}}{=} -c_1 x, \quad c_1 \in \mathbb{R}^+ \qquad\qquad \dot{\xi} = -c_1\dot{x} = -c_1 v, \\ \therefore \dot{V}_1 = -c_1 x^2 + xz. \end{aligned}$$

The virtual state error term, $z = v - \xi$, is now

$$z = v + c_1 x, \qquad\qquad \dot{z} = k[x-y]^2 + u + c_1 v.$$

Backstepping one integrator to incorporate $\dot{z}$, and hence the input u, a second control Lyapunov function is defined:

$$\begin{aligned} V_2 &\stackrel{\text{def}}{=} V_1 + \tfrac{1}{2}z^2, \\ \dot{V}_2 &= \dot{V}_1 + z\dot{z}, \\ &= [xz + x\xi] + z\left[u + k[x-y]^2 + c_1 v\right], \\ &= -c_1 x^2 + z\left[u + x + k[x-y]^2 + c_1 v\right]. \end{aligned}$$

The simplest route to stability is taken when the non-linearities are simply cancelled by the input control force, u:

$$\begin{aligned} u &\stackrel{\text{def}}{=} -c_2 z - x - k[x-y]^2 - c_1 v, \quad c_2 \in \mathbb{R}^+ \\ &= -x[c_1 c_2 + 1] - v[c_1 + c_2] - k[x-y]^2, \qquad (11) \\ \therefore \dot{V}_2 &= -c_1 x^2 - c_2 z^2 < 0 \;\forall\; x, z \neq 0 \qquad (12) \end{aligned}$$

For an ideal system, proof of global asymptotic stability of the controlled system follows from Eq. (12) [9].

This controller design is equivalent to feedback linearisation (note, *not* linearisation of the dynamics around the operating point as in Eq. (5)) since the choice for u simply cancels the nonlinearity and applies controller gains on the states x and v. Substituting Eq. (11) into Eq. (9) results in the closed loop system, for some controller gains c_1 and c_2,

$$\ddot{x} = -x[c_1 c_2 + 1] - \dot{x}[c_1 + c_2]\,. \tag{13}$$

Note that these closed loop dynamics are independent of the disturbance y. For an ideal system, attenuation is therefore infinite. However, errors will occur as the true dynamics deviate from the approximation used to derive the controller in Eq. (11). While these errors can lead to instability, increasing the controller gains c_1 and c_2 is sufficient to create a local region of stability around the nominal position that is large enough to contain the effects of the disturbance. It is possible, however, to design a more involved backstepping controller to compensate robustly for this problem.

An equivalent controller to Eq. (11) can be designed for the vertically repelling spring, resulting in identical closed loop dynamics (Eq. (13)). Referring to Figure 6, the two controllers are:

$$U_2 = -mx[c_1 c_2 + 1] - m\dot{x}[c_1 + c_2] - K[x - y]^2\,, \tag{14}$$

$$U_1 = \underbrace{-mx[c_1 c_2 + 1] - m\dot{x}[c_1 + c_2]}_{\text{Controller dynamics}} \underbrace{- K_3[x - y]^3 - K_2[x - y]^2 - K_1[x - y]}_{\text{Cancelation of open loop dynamics}}\,. \tag{15}$$

6 SIMULATION RESULTS

Results are obtained by investigating the dynamics in numerical simulation of the more conventional vertically repelling spring and the zero stiffness spring, both under equivalent forms of control, as derived in the previous section.

For the simulations to follow, the 'true' magnet dynamics are modelled using forces obtained from Eq. (2). The magnets are 20 mm cubes, and the zero stiffness spring is chosen to have a magnet gap (see Figure 1c) of 20 mm. Without loss of generality, the mass supported by the springs is chosen to be equal to the minima of the force vs. displacement curve of the zero stiffness spring, producing the zero stiffness condition. That is, mass $m = 1.836$ kg. For a different mass, a different gap would be chosen.

The disturbance input is assumed to be Gaussian-distributed random displacement with a standard deviation of 1 mm; this is numerically differentiated to obtain the input velocities for a linear damping of 5%, shown by d in Eq. (6). This damping term is included to approximate within an order of magnitude the real-world effects of air resistance and eddy currents.

Several simulations are presented with different controller gains. Initially, they are chosen to be large enough to overcome instability through the controller approximation errors given the specified input disturbance. Successively greater values were then selected to demonstrate the limits of the control performance. In total, simulations were performed for three sets of controller gains on each of the two springs with the controllers respectively shown in Eqs (14) and (15).

A summary of the results are shown in Table 1, tabulating RMS average values of displacement and force experienced by the support and the control force exerted to effect the control. The zero stiffness spring has both a greater vibration attenuation and an order of magnitude smaller control effort compared to the vertically repelling spring.

Figure 7 shows the vibration transmissibilities of the springs, calculated as the ratio between the output displacement and input disturbance power spectra. Power spectra ratios were used rather than frequency response functions (the ratio of the cross-spectra to output auto-spectra) due to the non-linear response.

Although the *ideal* closed loop dynamics should be equal (if the controller cancellations were perfect) and the displacements of the suspended magnet should tend towards zero, the mismatch between the estimated dynamics, Eqs (7) and (8), and actual dynamics, from Eq. (2), shows discrepancy between the two systems.

The lower control effort result can be considered a result of the fact that the zero stiffness spring simply needs to be stabilised to achieve vibration isolation, whereas the vertically repelling spring has dynamics that need to be actively cancelled to achieve the same result. The is very apparent for the high gain cases, where the control effect changes little for the zero stiffness spring from the lower gain case, but the isolation performance increases significantly. In comparison, the control effort of the vertically repelling spring increases fourfold.

6.1 Rejection of direct force disturbances

The second notable feature of the controller used is the behaviour of the closed loop dynamics, shown in Eq. (13). It has already been shown that greater control effort will correspond to greater vibration isolation from the ground. In addition, the natural frequency of the closed loop system, $\omega_n = \sqrt{c_1 c_2 + 1}$, will also increase. This will have the effect of increasing the attenuation of direct disturbance forces applied to the floating spring (for example, due to vibrations of machinery being supported or external excitation from turbulent airflow).

Table 1: RMS values of the displacements, total forces, and control forces on the two springs for increasing control gains c_1, c_2.

System			RMS values		
Spring	c_1	c_2	Disp. (mm)	Force (N)	Control (N)
Vertically repelling	20	10	0.376	2.04	2.14
	50	25	0.129	1.48	6.25
	100	50	0.042	1.32	8.20
Zero stiffness	20	10	0.146	0.197	0.142
	50	25	0.100	0.263	0.199
	100	50	0.006	0.201	0.167

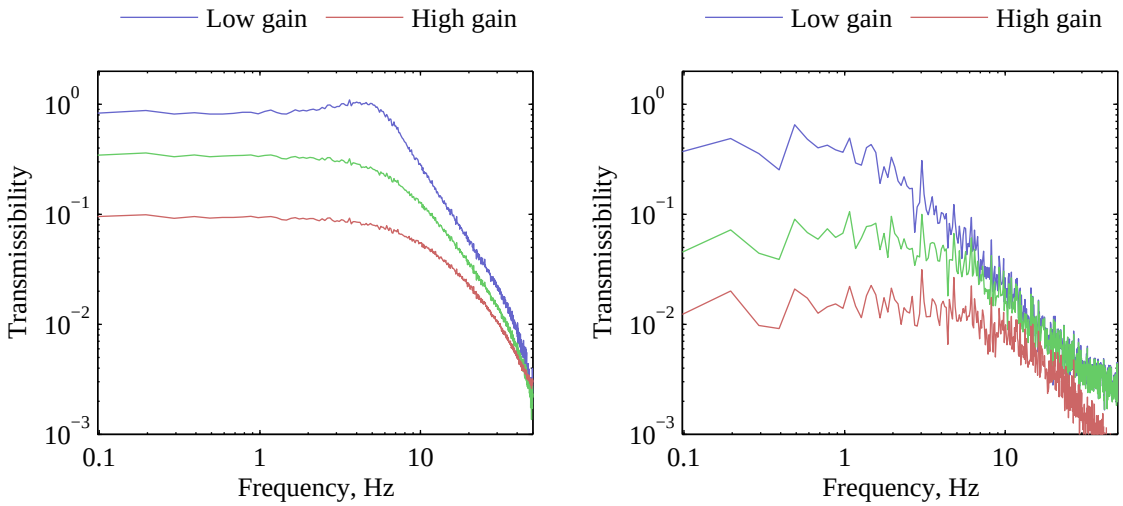

(a) Vertically repelling spring

(b) Zero stiffness spring

Figure 7: Transmissibilities of the actively controlled springs for various gains.

7 INHERENT ASSUMPTIONS

Many assumptions have been made to simplify the analyses in this paper. These assumptions will be lifted in the practical development of the vibration isolator. The zero stiffness property only holds when the magnet distances are tuned to support the mass of the isolator in the region of local force minima. Variations of the load would require a variable magnet separation distance, which could be effected with an actively controlled screw drive for (slow) online tuning.

The horizontal dynamics may be analysed and stabilised through similar analysis to that shown in this paper for the vertical direction. Alternatively, the spring may be constrained in the vertical direction.

It has been assumed here that the states of the system are fully observable. In practice, only the relative displacement $[x - y]$, relative velocity $[\dot{x} - \dot{y}]$, and the absolute accelerations $\ddot{x}$ and $\ddot{y}$ are directly measureable, but these parameters may be combined in an observer to obtain the required states used for feedback in this paper.

The effects of the actuator dynamics have not been modelled, nor have problems relating to achieving moment-free forces been addressed. With careful placement of zero stiffness voice-coil actuators, these problems should not be significant in practice.

8 SUMMARY

The unique force characteristic of a magnetic configuration combining vertically attracting and vertically repelling springs allows non-contact load bearing with zero stiffness properties. This is different from a classical spring that has a lower bound on its stiffness and hence a lower limit on its vibration isolation capabilities.

The non-linear force-displacement relationship of this combination spring required a non-linear controller, which was developed using a backstepping technique. Simulation results based on this controller displayed the zero stiffness tendency anticipated; smaller than unity transmissibility was achieved over the entire frequency spectrum.

REFERENCES

[1] S. Earnshaw, On the nature of the molecular forces which regulate the constitution of the luminiferous ether, Transactions of the Cambridge Philosophical Society, **3**(1), 97–112 (1842).

[2] L. Tonks, Note on Earnshaw's theorem, Electrical Engineering, **59**(3), 118–119 (1940).

[3] E. Puppin and V. Fratello, Vibration isolation with magnet springs, Review of Scientific Instruments, **73**(11), 4034–4036, URL `http://dx.doi.org/10.1063/1.1512325` (2002).

[4] G.-J. P. Nijsse, *Linear motion systems: a modular approach for improved straightness performance*, Ph.D. thesis, Delft University of Technology, URL `http://repository.tudelft.nl/file/80827/161960` (2001).

[5] J. T. Xing, Y. P. Xiong, and W. G. Price, Passive-active vibration isolation systems to produce zero or infinite dynamic modulus: theoretical and conceptual design strategies, Journal of Sound and Vibration, **286**(3), 615–636, URL `http://dx.doi.org/10.1016/j.jsv.2004.10.018` (2005).

[6] A. Carrella, T. P. Waters, and M. J. Brennan, Optimisation of a passive vibration isolator with quasi-zero-stiffness characteristic, ISVR Technical Memorandum No. 960, University of Southhampton (2006).

[7] G. Akoun and J.-P. Yonnet, 3D analytical calculation of the forces exerted between two cuboidal magnets, IEEE Transactions on Magnetics, **MAG-20**(5), 1962–1964 (1984).

[8] F. Bancel, Magnetic nodes, Journal of Physics D: Applied Physics, **32**, 2155–2161, URL `http://www.iop.org/EJ/abstract/0022-3727/32/17/304` (1999).

[9] H. K. Khalil, *Nonlinear Systems* (Macmillan, 1992).

[10] M. Krstić, I. Kanellakopoulos, and P. Kokotović, *Nonlinear and Adaptive Control Design* (John Wiley and Sons, 1995).